Comparative Biochemistry and Physiology, Part D 8 (2013) 334–343

Contents lists available at ScienceDirect

Comparative Biochemistry and Physiology, Part D

journal homepage: www.elsevier.com/locate/cbpd

Transcriptome responses in the rectal gland of fed and fasted spiny dogfish shark (*Squalus acanthias*) determined by suppression subtractive hybridization

Courtney A. Deck [a,b], Sheldon J. McKay [c], Tristan J. Fiedler [d], Christophe M.R. LeMoine [a,b], Makiko Kajimura [e,f], C. Michele Nawata [e,f], Chris M. Wood [e,f], Patrick J. Walsh [a,b,f,*]

[a] Department of Biology, University of Ottawa, Ottawa, ON K1N 6N5, Canada
[b] Centre for Advanced Research in Environmental Genomics, University of Ottawa, Ottawa, ON K1N 6N5, Canada
[c] Cold Spring Harbor Laboratory, Cold Spring Harbor, NY 11724, USA
[d] Department of Biological Sciences, Florida Institute of Technology, Melbourne, FL 32901, USA
[e] Department of Biology, McMaster University, Hamilton, ON L8S 4K1, Canada
[f] Bamfield Marine Sciences Centre, Bamfield, BC V0R 1B0, Canada

ARTICLE INFO

Article history:
Received 11 June 2013
Received in revised form 24 September 2013
Accepted 26 September 2013
Available online 6 October 2013

Keywords:
Elasmobranchs
Rectal gland
Transcript regulation
Feeding
Ion transport
Metabolism

ABSTRACT

Prior studies of the elasmobranch rectal gland have demonstrated that feeding induces profound and rapid up regulation of the gland's ability to secrete concentrated NaCl solutions and the metabolic capacity to support this highly ATP consuming process. We undertook the current study to attempt to determine the degree to which up regulation of mRNA transcription was involved in the gland's activation. cDNA libraries were created from mRNA isolated from rectal glands of fasted (7 days post-feeding) and fed (6 h and 22 h post-feeding) spiny dogfish sharks (*Squalus acanthias*), and the libraries were subjected to suppression subtractive hybridization (SSH) analysis. Quantitative real time PCR (qPCR) was also used to ascertain the mRNA expression of several genes revealed by the SSH analysis. In total the treatments changed the abundance of 170 transcripts, with 103 up regulated by feeding, and 67 up regulated by fasting. While many of the changes took place in 'expected' Gene Ontology (GO) categories (e.g., metabolism, transport, structural proteins, DNA and RNA turnover, etc.), KEGG analysis revealed a number of categories which identify oxidative stress as a topic of interest for the gland. GO analysis also revealed that branched chain essential amino acids (e.g., valine, leucine, isoleucine) are potential metabolic fuels for the rectal gland. In addition, up regulation of transcripts for many genes in the anticipated GO categories did not agree (i.e., fasting down regulated in feeding treatments) with previously observed increases in their respective proteins/enzyme activities. These results suggest an 'anticipatory' storage of selected mRNAs which presumably supports the rapid translation of proteins upon feeding activation of the gland.

1. Introduction

The elasmobranch rectal gland has fascinated physiologists for decades. Capable of secreting a nearly 0.5 M NaCl solution to its lumen (for eventual voiding via the lower intestine), it plays an important role in osmoregulation and has served as a key model for understanding trans-epithelial transport of ions. Especially in the spiny dogfish shark (*Squalus acanthias*), its utility has no doubt been aided by the relatively simple architecture of the gland and the ease with which both afferent and efferent blood vessels, and the gland's duct itself, can be cannulated for in vitro experimental manipulation. Indeed, studies have mapped out a now classic model where several plasma membrane-bound proteins, including Na^+K^+ ATPase, the 'CFTR' Cl^- channel, and $Na^+K^+2Cl^-$ transporters, are coordinated to excrete salt (Silva et al., 1997; Olson, 1999; Anderson et al., 2007). Previous findings also included the demonstration of several potential natural and artificial signals for activation of the gland (e.g., C-type natriuretic peptide (CNP); vasoactive intestinal peptide (VIP), forskolin, etc.) (Epstein et al., 1983; Schofield et al., 1991). While originally it was believed that the gland functioned continuously to aid in overall osmoregulatory balance, more recently it has been shown that the gland is relatively inactive during frequent bouts of fasting, but becomes highly active very shortly after feeding; notably dogfish feed opportunistically, and therefore sporadically, in the wild (see references contained within Wood et al., 2010 for review).

The activation of the gland by feeding has been studied from a number of perspectives: morphological, physiological, metabolic, biochemical, and proteomic (for review, see Wood et al., 2010). These studies lead to an integrated view that: (i) feeding and digestion trigger activation of the gland, with at least one of the key signals being the increase in plasma pH associated with acid-secretion to the stomach

* Corresponding author at: Dept. of Biology, 30 Marie Curie, University of Ottawa, Ottawa, ON K1N 6N5, Canada. Tel.: +1 613 562 5800x6328; fax: +1 613 562 5486.
E-mail address: pwalsh@uottawa.ca (P.J. Walsh).

1744-117X/$ – see front matter
http://dx.doi.org/10.1016/j.cbd.2013.09.003

(the so-called 'alkaline tide') (Wood et al., 2005; Shuttleworth et al., 2006; Wood et al., 2007a,b), while another may be the plasma volume expansion that accompanies the ingestion of salty food and accompanying seawater (Solomon et al., 1984; Silva et al., 1997); (ii) morphologically, the gland transitions from a 'dormant' (somewhat apoptotic) state, to a highly active secretory morphology (Matey et al., 2009), accompanied by increases in amounts of key cytoskeletal/muscular proteins (e.g., transgelin, tropomyosin) (Dowd et al., 2008); (iii) likewise, amounts and activities of key proteins of the ion transport pathway are up regulated, including Na^+K^+-ATPase and voltage-dependent anion channels (MacKenzie et al., 2002; Walsh et al., 2006; Dowd et al., 2008); (iv) the metabolic rate of the gland increases markedly, with a relatively complex pattern of metabolic pathway dependence (Walsh et al., 2006; Dowd et al., 2008). While glucose appears to be the main fuel source, evidence exists that β-hydroxybutyrate can serve as an auxiliary fuel (at least in the early stages of activation). Furthermore, although the gland appears to be a highly aerobic tissue with high densities of mitochondria, and high activities of tricarboxylic acid (TCA) cycle and energy production enzymes (e.g., isocitrate dehyrogenase, citrate synthase, ATP synthase) that increase in activity upon feeding, it is likely that at least some of its energy comes from anaerobic glycolysis as evidenced by large increases in lactate dehydrogenase activity when the gland is activated. The inability of lactate to fuel the gland at least in vitro (Walsh et al., 2006) argues against the increase in LDH being for lactate oxidation.

The above picture has been developed using several tools, and leads to a relatively 'straightforward' view of the gland's activation involving changes in morphology, ion secretion, and supporting metabolic pathways. The time course of changes (especially protein concentrations and enzyme activities), many of which were elevated after only 6 h post-feeding, was consistent with either a coordinated increase in both transcription and translation for appropriate genes, or rapid translation of pre-existing message (Dowd et al., 2008). With this background in mind, we undertook a study of the response of the transcriptome of the gland to feeding/fasting in order to test the hypothesis that widespread transcriptomic responses occur rapidly and agree with the physiological activation of the rectal gland upon feeding. Our null hypothesis is that a transcriptomic response was not a large part of the gland's activation in the short-term. Furthermore, assuming at least some role for transcriptional activation, we wished to gain insight into aspects of the activation of the gland that might have been overlooked by prior approaches.

For this examination, we used the approach of suppression subtractive hybridization (SSH), in which the mRNA (converted to cDNA) population of a 'tester' sample (e.g., rectal gland tissue from a fed dogfish) is hybridized with an excess of mRNA from a 'driver' sample (e.g., rectal gland tissue from a fasted dogfish), such that the mRNA transcripts in common are subtracted from the tester, enriching the tester sample for its unique transcripts. The SSH approach (Diatchenko et al., 1996), although not without its biases, has proven to be a useful tool in complementary studies to traditional physiological and metabolic biochemistry approaches, including many studies in comparative biology (Gracey et al., 2001; Fiol et al., 2006).

2. Materials and methods

2.1. Animals and feeding protocols

Males of the spiny dogfish shark (*Squalus acanthias suckleyi*) were captured by angling or trawl in Barkley Sound, BC (Canada) offshore from Bamfield Marine Sciences Centre in June, 2007 and 2009 and August 2012 under various permits from the Canadian Department of Fisheries and Oceans. Note that Ebert et al. (2010) have recently proposed that these north-east Pacific dogfish may be a separate species (*Squalus suckleyi*) rather than a subspecies of *S. acanthias*. Consistent with our prior feeding experiments (see Wood et al., 2010), fish were maintained in a 155,000 L circular tank supplied with running seawater and aeration. After acclimation to the tank, dogfish fed voraciously on a diet of frozen hake supplied every 4th day to a ration size of approximately 2.5% body weight. At 6 h, 22 h (48 h for qPCR only), and 7 days post-feeding (this latter group was removed to a separate tank to ensure that additional feeding did not take place, and is referred to as 'Fasted' below), dogfish were sacrificed by overdose of MS-222 (1 g/L) and the rectal glands removed, frozen in liquid nitrogen and stored at −80 °C. Feeding status was confirmed by examining the gut for the presence (or absence) of food. All experiments were conducted in accordance with guidelines of the Canadian Council of Animal Care, and under approvals from the Animal Care Committees of the University of Ottawa, McMaster University and the Bamfield Marine Sciences Centre.

2.2. Isolation of RNA and construction of a normalized cDNA library

A normalized cDNA library from dogfish rectal gland was created in order to form a potential basis for comparison to the distribution of genes identified (e.g., Gene Ontology (GO) analysis categorization) from more specific treatments by the SSH approach. Total RNA was isolated by standard Trizol (Invitrogen, Grand Island, NY, USA) extraction methods from individual rectal gland samples from 6 fish each from the 6 h, 22 h and 'Fasted' treatments and the RNA integrity was verified with a BioAnalyzer 2100 (Agilent, Mississauga, ON, Canada). Equal amounts of total RNA from these 18 fish were pooled to yield a single sample from which polyA mRNA was further purified by a magnetic bead-based method (Ambion Poly(A)Purist MAG, Ambion, Austin, TX, USA). A normalized cDNA library was created using the Creator SMART cDNA Construction Kit (Clontech, Mountain View, CA, USA) and CDS-3M Adaptors in the Trimmer Direct cDNA Normalization Kit (Evrogen, Moscow, Russia); following normalization, *Sfi*I digestion, and size fractionation, cDNA was directionally inserted into a pTB vector, and transformed into *Escherichia coli* via electroporation. Bacteria were grown on LB agar plates with carbenicillin (50 μg/mL), and individual colonies were hand-picked at random and grown overnight at 37 °C in LB medium with carbenicillin. PCR was performed directly on 1 μL aliquots of this broth (using primers against the arms of the pTB vector) and PCR products cleaned and sequenced on an ABI 3730xl sequencer (using slight modifications of the methods from Oleksiak et al., 2001).

2.3. Construction of SSH libraries

Equal quantities of total RNA from the above samples of 18 glands were pooled (6 fish per pool) into three samples each representing 6 h, 22 h and 'Fasted' treatments and mRNA was purified as above. Tester and Driver cDNA was synthesized and adaptor-ligated, and subtractions performed as per instructions in the PCR-Select cDNA Subtraction Kit (Clontech). Six libraries were created representing forward and reverse subtractions for the three treatments (letters correspond to those in tables in Results and discussion): (A) fasted minus 6 h; (C) 6 h minus fasted; (E) fasted minus 22 h; (G) 22 h minus fasted; (I) 6 h minus 22 h; and (K) 22 h minus 6 h. PCR products from second amplifications were cloned into pCR2.1 TOPO vector (Invitrogen), transformed into *E. coli*, and colonies were hand-picked, grown in liquid broth overnight at 37 °C and PCR and sequencing was performed as above, except that primers were to the M13R and M13F(-20) sites of this vector.

2.4. Sequence analysis and annotation

Much of the analysis was similar to that conducted in a prior study by our group on transcriptome variation in *Aplysia* sp. (Fiedler et al., 2010). We have defined quality ESTs as sequence reads with length ≥100 bp after trimming of low quality (phred score < 20) ends, and vector sequence removal using cross_match (Ewing and Green, 1998;

Ewing et al., 1998). ESTs were clustered separately for each of the seven rectal gland libraries using CAP3 (Huang and Madan, 1999). We refer to the clustered ESTs as contigs, after the definition of Staden (1980), which comprised both clustered EST and un-clustered singletons. Contigs were subjected to BLAST analysis (NCBI BLAST; Altschul et al., 1997) against protein and sequence databases using ad hoc Perl scripts based on the BioPerl programming interface (Stajich et al., 2002) to run BLAST analysis.

In order to identify matches with previously published EST sequences, individual ESTs were BLASTed against the subset of dbEST (Boguski et al., 1993) that excluded human and mouse ESTs. The tBLASTx (translated nucleotide against translated nucleotide) program was used to identify more distantly related ESTs. An expect-value cutoff of 1e−8 was used as the retention criterion for BLAST hits (see below for discussion of this cutoff). GO and KEGG annotations were performed with the annot8r software package (Schmid and Blaxter, 2008). As part of this analysis, contigs from all libraries were BLASTed against subsets of UniProt (The UniProt Consortium, 2008) databases optimized for identification of Gene Ontology (GO, The Gene Ontology Consortium, 2000) or KEGG pathways (Kanehisa et al., 2008) using the program BLASTx (translated nucleotide against protein). As suggested in the program documentation, the expect-value cutoff of 1e−8 was used for retention of BLAST matches. The top 10 best hits for each EST were used to assign GO_slim terms and KEGG pathways.

Contigs were also used for BLAST analysis against the complete Uniprot Knowledgebase (Swissprot and TREMBL) protein databases with the BLASTx program. In order to get a general sense of which EST clusters matched annotated proteins, we retained up to the top 10 BLAST hits for each contig that met the expect-value cutoff of 1e−8 as recommended in Schmid and Blaxter (2008). The higher quality annotations in Swissprot were preferentially retained, and TREMBL was consulted only where 10 Swissprot hits were not found. The taxonomic ranks Kingdom, Phylum and Class (or nearest equivalent) of these BLAST hits were identified by recursion through a local copy of the NCBI taxonomy database (Wheeler et al., 2000).

2.5. Real time quantitative PCR

In order to determine the validity of the SSH approach in this system, real time PCR (qPCR) was conducted. We quantified the relative amounts of transcripts for selected genes that appeared to change with treatment in the SSH libraries, notably lactate dehydrogenase, cytochrome C oxidase, glutamine synthetase, and Na^+K^+ ATPase. Since RNA from the original SSH libraries created in 2007–2009 had degraded by this point in our study, we obtained new samples in 2012. Due to permit restrictions, and the need to coordinate sampling with other investigators of ongoing studies to reduce fish use, the time points of some of these new samples do not exactly coincide with those obtained for the SSH libraries (i.e., in some cases 6 h points were not available and 48 h points were added). Nonetheless, they represent key pre- and post-feeding junctures identified in prior research (Walsh et al., 2006; Dowd et al., 2008). Total RNA was extracted from the glands using Trizol reagent (Invitrogen) according to the manufacturer's instructions, treated with DNase I (Invitrogen), and used as a template for reverse transcription (RT). The RT reactions combined 2 mg RNA (quantified spectrometrically by NanoDrop) with 375 ng random hexamers (Integrated DNA Technologies), 125 ng oligo dTs (IDT), and dNTPs (Invitrogen; 0.5 mM final concentration) and incubating the mixture at 65 °C for 5 min. The reaction was then chilled on ice for 5 min and first-strand reaction buffer (Invitrogen; 1× final concentration), dithiothreitol (5 mM final concentration), RNase Out (Invitrogen; 0.5 μL), and nuclease-free water (0.5 μL) were added. The mixture was incubated at 42 °C for 2 min and then combined with Superscript II reverse transcriptase (Invitrogen; 1 μL) to a total volume of 20 μL. Lastly, the reaction was incubated at 42 °C for 50 min and then 72 °C for 15 min.

Following RT, the cDNA encoding each of the chosen genes was cloned to sequence verify the amplicons by adding 1 μL of diluted template (1:5) to a 25 μL total volume containing PCR reaction buffer (Denville Scientific; 1× final concentration), dNTPs (0.2 mM final concentration), 0.15 μL Choice Taq (Denville Scientific), and sense and antisense primers (0.2 mM final concentrations). Primers for each gene were derived from existing *S. acanthias* sequences where applicable (Supplementary Table 1). The cycling parameters were 94 °C for 30 s followed by 40 cycles of 94 °C for 30 s, 60 °C for 30 s, and 72 °C for 30 s and concluding with 15 min at 72 °C. The products were visualized on a 2% agarose gel and the amplicons gel purified and spliced into a pDrive Cloning Vector (Qiagen). The vectors were subsequently cloned using Subcloning Efficiency DH5α Competent Cells (Invitrogen), purified, and sequenced using the M13F primer.

For qPCR, 1 μL of the diluted cDNA template was added to a 12.5 μL total volume containing 6.25 μL Rotor-Gene SYBR Green PCR master mix (Qiagen) and 200 nM each gene specific sense and antisense primer. Relative mRNA levels for each gene of interest were normalized to *S. acanthias* EF1α levels. Fluorescence was detected using a Rotor-Gene Q Real Time PCR cycler with the following cycling parameters: 95 °C for 5 min followed by 40 cycles of 95 °C for 5 s and 60 °C for 10 s. All reactions were run in duplicate and relative mRNA levels were calculated using the δ Ct method. Statistics on these values were by one-way ANOVA and Holm-Sidak post-hoc test.

3. Results and discussion

In this study, we produced Normalized and SSH libraries in order to investigate mRNA transcript responses to feeding and fasting in the rectal gland of *S. acanthias*. Information on aspects of sequencing and contig creation appear in Supplementary Tables 2 and 3, and unedited results of blast hits from these seven libraries appear in Supplementary Table 4. Sequences for these Contigs are available in Supplementary File A.

Since one potential bias of the SSH approach is that highly abundant transcripts may 'leak' through the subtraction process, we transformed the data to remove potential false positives from the SSH libraries (Supplementary Table 5); a false positive was suspected and removed when a given gene appeared as up regulated in both the forward and reverse library subtractions. These edited lists were then utilized for GO and KEGG (Kyoto Encyclopedia of Genes and Genomes) pathway analyses, the results of which appear in Table 1 and Fig. 1, and Table 2, respectively. Notable biological processes being represented include metabolic processes and regulation, transport, and cell death, while the KEGG analysis revealed pathways involved in the progression of neurodegenerative diseases. In addition to these analyses, we further condensed the number of genes of interest from the SSH lists by removing duplicately named genes (e.g., different EST hits for the same basic gene) (Table 3a, b). We also conducted qPCR on four genes representing various biological pathways in order to complement the SSH approach (Figs. 2 and 3).

3.1. General overview

A total of 170 transcripts were up regulated in the various treatments, 67 of which were up regulated by feeding treatments (Libraries C, G, I and K), and 63 of which were up regulated by fasting treatments (Libraries A and E) (Supplementary Table 5). Of the GO categories, those of 'Biological Process' are the most interesting. The largest changes in transcript abundances relative to both fasting and the normalized library are in the sub-categories of 'Metabolic Process' and 'Transport' (Table 1 and Fig. 1). This result is not surprising given the main function of the rectal gland is to secrete NaCl and that it is an energetically expensive process. This result is also consistent in general with prior observations at the enzymatic/proteomic level (Walsh et al., 2006; Dowd et al., 2008). Furthermore, the role of structural proteins during activation of the gland as initially revealed in proteomic studies (Dowd et al., 2008)

Table 1
Total number of EST identifications that are up regulated between time points in each Gene Ontology category in the rectal glands of fasted (F) and fed (6 h, 22 h) dogfish sharks (*Squalus acanthias*). Letters refer to the SSH libraries listed in Materials and methods.

GO_slim term	Total	Norm	A (F-6 h)	C (6 h-F)	E (F-22 h)	G (22 h-F)	I (6 h-22 h)	K (22 h-6 h)
Cellular component								
Intracellular (GO:0005622)	568	239	89	72	21	68	12	67
Membrane (GO:0016020)	373	148	52	39	15	32	10	77
Cell (GO:0005623)	40	9	6	4	2	3	1	15
Extracellular region (GO:0005576)	33	9	8	1	10	2	0	3
Biological process								
Metabolic process (GO:0008152)	311	101	57	51	16	44	6	36
Transport (GO:0006810)	196	92	26	17	6	18	5	32
Regulation of biological process (GO:0050789)	190	43	36	31	11	7	0	62
Nucleobase-containing compound metabolic process (GO:0006139)	126	59	20	8	8	14	7	10
Multicellular organismal development (GO:0007275)	104	24	3	4	14	3	1	55
Response to stimulus (GO:0050896)	71	32	8	6	9	7	0	9
Cellular process (GO:0009987)	70	32	14	4	1	7	1	11
Cell differentiation (GO:0030154)	31	7	1	1	1	2	0	19
Cell death (GO:0008219)	12	7	1	2	0	0	0	2
Cell communication (GO:0007154)	3	0	1	0	0	0	0	2
Extracellular structure organization (GO:0043062)	2	0	0	0	1	0	0	1
Cellular membrane fusion (GO:0006944)	2	2	0	0	0	0	0	0
Cellular component movement (GO:0006928)	2	0	1	0	0	0	1	0
Molecular function								
Binding (GO:0005488)	533	211	114	50	29	49	10	70
Catalytic activity (GO:0003824)	134	61	30	6	2	17	4	14
Oxidoreductase activity (GO:0016491)	88	24	13	13	5	20	0	13
Transporter activity (GO:0005215)	70	31	10	10	0	3	6	10
Transferase activity (GO:0016740)	45	22	12	7	0	1	0	3
Structural molecule activity (GO:0005198)	31	13	3	6	2	2	1	4
Enzyme regulator activity (GO:0030234)	18	2	8	4	3	0	0	1
Ligase activity (GO:0016874)	17	5	2	0	4	6	0	0
Regulation of biological process (GO:0050789)	15	5	4	1	1	0	0	4
Isomerase activity (GO:0016853)	12	2	2	2	0	4	0	2
Nucleobase-containing compound metabolic process (GO:0006139)	10	2	3	2	1	0	0	2
Motor activity (GO:0003774)	4	2	1	0	0	0	0	1
Lyase activity (GO:0016829)	3	0	0	2	0	1	0	0
Signal transducer activity (GO:0004871)	1	0	0	0	0	1	0	0

is confirmed and expanded by the current results (Table 3a,b), as well as the role of apoptosis/cell death (Table 3a,b) as initially hypothesized from morphological studies (Matey et al., 2009). There were also changes in transcripts from a number of other sub-categories that fit well with a dynamically coordinated regulation of gene transcription/translation (e.g., Process Regulation, RNA Processing, Transcription, Translation, etc.) (Table 3a,b). However, there were a number of other categories of interest, as well as incidences of unanticipated genes up regulated in treatments. These interesting points, as well as further details on some of the anticipated changes, will be discussed in more detail in the following sections that are based on some of the above sub-categories.

3.2. Cellular metabolism

The GO term analysis revealed that a large percentage of the genes from the SSH libraries are involved in metabolic processes and there appears to be a general up regulation of such genes with feeding (Fig. 1). Due to the aerobic nature of the rectal gland and the hypothesis that it may resort to anaerobic metabolism during times of peak activity (Walsh et al., 2006), we selected a gene involved in each of these pathways with which to conduct qPCR. Cytochrome C oxidase (CCO) is an enzyme involved in aerobic metabolism that typically correlates with mitochondrial oxidative capacity. The SSH libraries developed in this study indicate an up regulation of the mRNA for this gene with feeding (Table 3a), which correlates well with previous observations that feeding promotes increased development of mitochondria in the rectal gland (Matey et al., 2009) and increases in mitochondrial enzyme activities (Walsh et al., 2006). qPCR for this gene confirmed a significant up regulation of CCO mRNA by 22 h post-feeding as seen in Fig. 2B.

LDH is an indicator of anaerobic pathway capacity and the activity of this enzyme at ~130 units/g wet mass is reasonably high even in fasted dogfish rectal glands (Walsh et al., 2006). This activity also increased significantly at 6 h and 20 h post-feeding (Walsh et al., 2006). The increase in activity appears to be at least partly supported by increased transcription as we observed an up regulation of transcripts for this enzyme in the SSH libraries of both 6 and 22 h minus fasted, although no difference between 6 and 22 h (Table 3). A trend toward up regulation of transcripts at 22 and 48 h was further supported by qPCR methods (Fig. 3B), although the time points do not directly correspond to the SSH samples.

SSH also revealed a number of genes up regulated at 22 h post feeding associated with branch chain amino acid catabolism (Table 3a). In particular, the transcripts of enzymes involved in the catabolism of valine (methylmalonate-semialdehyde dehydrogenase, propionyl-CoA carboxylase beta chain and isobutyryl-CoA dehydrogenase), isoleucine and leucine (methylmalonate-semialdehyde dehydrogenase) were enriched in the 22 h library (Table 3a). Interestingly, the plasma concentration of these three essential amino acids rapidly rise following a meal in dogfish, but start declining 30 h post feeding (Wood et al., 2010). Thus, this increase in transcripts for genes coding for amino acid catabolic enzymes detected by the SSH at 22 h concomitant with high circulating levels of these amino acids in the blood suggest that the gland increases its capacity to metabolically rely on these amino acids as a secondary metabolic response to a feeding event. Walsh et al. (2006) had previously concluded a small role for amino acids as fuels for the rectal gland, but this was based on the inability of alanine

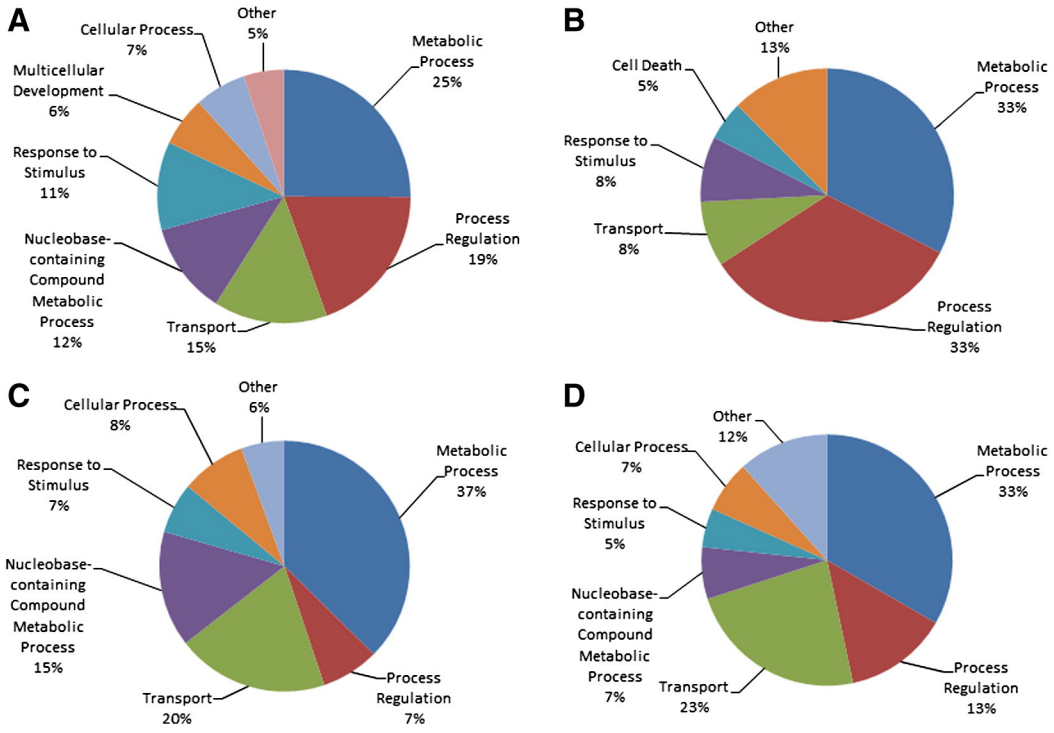

Fig. 1. Pie charts of categories of genes identified from rectal glands of fed and fasted spiny dogfish (*Squalus acanthias*) from the 'Biological Function' heading in GO analysis for (A) the NORM library, and SSH libraries from the following treatments: (B) 6 h minus 7 day fasted, (C) 22 h minus 7 day fasted, and (D) 22 h minus 6 h.

and glutamine to stimulate salt secretion. It would be of interest to test the ability of these essential amino acids to fuel rectal gland metabolism and salt secretion.

Another metabolic enzyme that was of interest to us was glutamine synthetase (GS) as it is responsible for trapping ammonia nitrogen to be used in urea (osmolyte) synthesis. Changes in activities of GS in the rectal gland are similar to those observed for LDH in that there is more than a doubling of GS activity at 6 and 20 h compared to fasted or 30 and 48 h post feeding (Walsh et al., 2006). This increase in GS activity at times of peak gland activity makes sense in terms of the need to scavenge ammonia for urea synthesis, especially in light of the above proposed role for essential amino acids as metabolic fuels. Therefore it was surprising that we observed an up regulation of transcripts for this enzyme with *fasting* in the SSH libraries, a result that was confirmed by qPCR (Fig. 2A). Matey et al. (2009) noted that it was not uncommon to observe cells in the early stages of apoptosis in fasted rectal glands, so this tissue may be releasing ammonia by protein degradation. Since during fasting, dogfish are extremely limited in the amount of nitrogen

Table 2
Total number of EST identifications that are up regulated between time points in each KEGG pathway in the rectal glands of fasted (F) and fed (6 h, 22 h) dogfish sharks (*Squalus acanthias*). Letters refer to the SSH libraries listed in Materials and methods.

KEGG pathway	Total	Norm	A (F-6 h)	C (6 h-F)	E (F-22 h)	G (22 h-F)	I (6 h-22 h)	K (22 h-6 h)
Parkinson's disease [ko:05012]	49	26	4	5	1	4	1	8
Huntington's disease [ko:05016]	48	28	2	5	1	3	1	8
Oxidative phosphorylation [ko:00190]	46	24	4	4	1	4	1	8
Alzheimer's disease [ko:05010]	42	24	2	5	1	3	1	6
Cardiac muscle contraction [ko:04260]	26	16	3	2	0	1	0	4
Ribosome [ko:03010]	21	11	1	4	1	2	1	1
RNA transport [ko:03013]	10	4	3	1	1	0	0	1
Pyruvate metabolism [ko:00620]	9	0	2	2	1	3	0	1
Propanoate metabolism [ko:00640]	8	1	0	2	0	5	0	0
Mineral absorption [ko:04978]	7	4	3	0	0	0	0	0
Viral myocarditis [ko:05416]	7	2	1	1	0	2	0	1
Glycolysis/gluconeogenesis [ko:00010]	7	0	2	2	0	2	0	1
Protein processing in endoplasmic reticulum [ko:04141]	6	4	0	0	1	0	0	1
Toxoplasmosis [ko:05145]	6	3	0	2	0	0	0	1
Pathways in cancer [ko:05200]	6	3	1	1	0	0	0	1
Valine [ko:00280]	6	1	0	1	0	3	0	1
Citrate cycle (TCA cycle) [ko:00020]	6	0	1	1	1	2	0	1
Carbon fixation in photosynthetic organisms [ko:00710]	6	0	2	1	1	1	0	1
Purine metabolism [ko:00230]	5	3	2	0	0	0	0	0
Endocytosis [ko:04144]	5	1	2	0	0	0	0	2
Spliceosome [ko:03040]	5	2	0	1	0	1	0	1
Focal adhesion [ko:04510]	5	0	2	0	1	1	0	1
Phagosome [ko:04145]	5	2	1	0	0	1	0	1
Glyoxylate and dicarboxylate metabolism [ko:00630]	5	0	0	1	1	2	0	1
Arginine and proline metabolism [ko:00330]	5	2	1	1	0	1	0	0

they can devote to urea synthesis, procuring nitrogen from degrading tissues may be what allows them to maintain their plasma urea levels during these periods, as observed in prior studies (Haywood, 1973; Armour et al., 1993; Kajimura et al., 2008). Glutamine supply from an active tissue like the rectal gland would be one source for urea synthesis, thus creating the need for modest GS activity even as the gland is deactivated (notably an enzyme of the Ornithine-Urea Cycle, ornithine carbamoyltransferase, is up regulated by feeding (Table 3a) indicating that at least a partial cycle might be operating in the rectal gland). There may be enhanced degradation of protein in general in the fasted rectal gland, and a higher standing stock of GS mRNA relative to fed fish may be required to sustain even this modest level of GS activity. The above results serve to reinforce the cautionary note that transcript abundances are not always reflected in enzyme activity, even in an enzyme like GS that is not believed to be subjected to post-translational modification of activity.

The above results for GS transcripts are mirrored in a more general way for many metabolic genes in that transcripts for 12 metabolic genes, many of them mitochondrial, are up regulated during fasting (Table 3b), a point we will return to below.

3.3. Ion transport

Secretion by the rectal gland is largely dependent on the ability to transport various ions across both the apical and basolateral membranes, thus it was not surprising to see that this process was heavily represented in the SSH libraries (Fig. 1). One gene of particular interest was Na^+K^+-ATPase because: i) its activity is required to create gradients necessary for the entry of chloride into the cell and paracellular transport of Na^+; and ii) previous studies have shown increases in its activity post-feeding (Mackenzie et al., 2002; Walsh et al., 2006). In light of these observed increases in enzyme activity, it was surprising to find that the mRNA for this gene was down regulated with feeding according to the SSH libraries (Table 3b). In order to investigate this further, we conducted qPCR and the results indicated no significant differences between the rectal glands from fed and fasted dogfish (Fig. 3A). This investigation of Na^+K^+-ATPase mRNA levels was focused on the alpha subunit as this is what appeared in the SSH libraries. Little is known about the presence of different isoforms of this gene in elasmobranchs, or of the abundance of other subunits. In the teleost gill however, numerous studies have investigated the abundance of various alpha subunit isoforms and their relation to overall enzyme activity. Richards et al. (2003) determined that, upon transfer to sea water, there was a decrease in Na^+K^+-ATPase alpha 1a mRNA and an increase in alpha 1b mRNA in the gills of *Oncorhynchus mykiss* and these changes were accompanied with an increase in overall Na^+K^+-ATPase enzyme activity. Similar results were found by Bystriansky et al. (2006) in the gills of three salmonid species (*Salmo salar*, *O. mykiss*, *Salvelinus alpinus*). It is possible that *S. acanthias* also possesses multiple isoforms for the alpha subunit which could help explain the disconnect between Na^+K^+-ATPase activity and the mRNA levels observed in this study. However, Mahmmoud et al. (2000) previously discovered an FXYD domain-containing protein in the rectal gland of *S. acanthias*. These proteins are substrates for protein kinase C and have been shown to dissociate from the α-subunit of Na^+K^+-ATPase when phosphorylated, activating the enzyme (Mahmmoud et al., 2000). Thus, these proteins act as tissue-specific regulators of Na^+K^+-ATPase and may provide an alternate explanation for the aforementioned disconnect.

3.4. Morphology

It has previously been determined that the rectal gland undergoes significant changes in morphology when switching to its active state. During fasting, the gland's muscle and epithelial layers thicken and many cells enter the early stages of apoptosis (Matey et al., 2009). Upon feeding, this thickening is reversed in order to increase the lumen diameter and thus a significant amount of tissue remodeling is expected to occur. The SSH libraries indicate an increase in cell death at 6 h post-feeding, as seen in Fig. 1. This result appears to be counter-intuitive, however it is likely that allowing cells in the early stages of apoptosis to die off and subsequently increasing cell proliferation to allow tissue remodeling is more efficient than trying to reverse apoptosis as is the case in Burmese pythons, another species known to go for extended periods without feeding (Lignot et al., 2005; Helmstetter et al., 2009). These studies on the python gastrointestinal tract have shown that feeding induces cellular replication and extensive remodeling of the intestinal mucosa. This increase in cell death observed in the dogfish post-feeding could also explain the increases in GS activity observed by Walsh et al. (2006) as there will be a greater need to scavenge nitrogen from the degrading proteins at this time.

The SSH libraries revealed a few specific genes that are involved in apoptotic and cell proliferation pathways, one of which is the voltage-dependent anion channel (VDAC). Dowd et al. (2008) found an increase in VDAC protein levels at both 6 and 20 h post-feeding and in this study the SSH libraries revealed an increase in mRNA levels at 22 h (Table 3a). This protein forms a pore in the outer mitochondrial membrane and is said to be involved in allowing the mitochondrial contents that initiate apoptosis to leak out into the cytoplasm. A programmed cell death protein also appears at 22 h (Table 3a) suggesting that the rectal gland begins preparing to re-enter its dormant state shortly following a meal, possibly to minimize extra energy expenditures. Another interesting finding was the presence of a butyrate response factor in the fasted glands (Table 3b). This protein is a transcription factor that regulates the cell's response to growth factors, playing a role in cell proliferation. Its appearance in the fasted glands likely has to do with the extensive remodeling that is required to produce the dormant state, acting to prepare the gland for its next feeding period.

Another notable gene whose mRNA was up regulated in fasting was the iron storage protein ferritin (Table 3b). Perhaps some of the iron generated from the degradation of heme-containing respiratory chain proteins is being sequestered within the rectal gland so as to enable rapid resynthesis of these proteins as needed upon feeding activation.

3.5. Oxidative stress

The rectal gland is a highly aerobic tissue, taking up 95% of the oxygen from the blood it is perfused with (Solomon et al., 1984). Thus, one would expect the production of large amounts of reactive oxygen species (ROS), particularly during peak levels of activity when blood (and thus oxygen) supply to the gland is expected to increase. An interesting finding that resulted from our KEGG pathway analysis (Table 2) was the number of genes associated with neurodegenerative diseases, which are often characterized by the inability of the neurons to neutralize ROS. One interesting gene in particular to show up regulation during feeding was dna-J (Table 3a). This gene is a molecular chaperone that is believed to play a role in neutralizing ROS and it is one of the genes that are known to be affected in Parkinson's disease. Dna-J shows up in the SSH libraries at 22 h (Table 3a), which is after the gland's activity levels (and likely ROS production) have peaked. Thus, it is possible that this gene is playing a role in the gland's response to oxidative stress. Notably, another gene typically associated with stress (HSP 71) was also up regulated by feeding (Table 3a).

It was previously mentioned that LDH activity in the rectal gland is already high in fasted fish and yet this still increases post-feeding, along with mRNA levels. Although one explanation is that this increase is responsible for maintaining activity levels when the gland's activity is outpacing oxygen delivery, another possible explanation is that it is serving to reduce the production of ROS by anaerobically converting pyruvate to lactate rather than oxidizing it. Thus, the enzyme may be responsible for helping to regulate the amount of oxidative stress to which the gland is exposed.

Table 3
Lists of EST identities for Contigs from 7 SSH libraries grouped by Gene Ontology 570 category for rectal glands of (A) fed and (B) fasted dogfish sharks (*Squalus acanthias*). Letters 571 refer to the SSH libraries listed in Materials and methods.

Contig	Gene Ontology	Accession number	Description
a			
RG_G_Contig23	Metabolic	E1BFG0	Alpha-aminoadipic semialdehyde dehydrogenase OS = *Bos taurus* GN = ALDH7A1 PE = 2 SV = 3
RG_G_Contig9	Metabolic	Q5TI65	Brain protein 44 OS = *Homo sapiens* GN = BRP44 PE = 1 SV = 1
RG_G_Contig31	Metabolic	P21158	C-factor OS = *Myxococcus xanthus* GN = csgA PE = 1 SV = 1
RG_G_Contig21	Metabolic	Q9ZZ52	Cytochrome c oxidase subunit 1 OS = *Squalus acanthias* GN = MT-CO1 PE = 3 SV = 1
RG_G_Contig26	Metabolic	Q9ZZ48	Cytochrome c oxidase subunit 3 OS = *S. acanthias* GN = MT-CO3 PE = 3 SV = 1
RG_G_Contig18	Metabolic	Q96KP4	Cytosolic non-specific dipeptidase OS = *H. sapiens* GN = CNDP2 PE = 1 SV = 2
RG_G_Contig53	Metabolic	P79345	Epididymal secretory protein E1 OS = *B taurus* GN = NPC2 PE = 1 SV = 1
RG_G_Contig6	Metabolic	Q4R4W5	Isopentenyl-diphosphate delta-isomerase 1 OS = *Macaca fascicularis* GN = IDI1 PE = 2 SV = 2
RG_G_Contig76	Metabolic	Q9YI05	L-lactate dehydrogenase B chain OS = *S. acanthias* GN = ldhb PE = 2 SV = 1
RG_G_Contig19	Metabolic	Q02252	Methylmalonate-semialdehyde dehydrogenase [acylating]; mitochondrial OS = *H. sapiens* GN = ALDH6A1 PE = 1 SV = 2
RG_G_Contig16	Metabolic	Q2TBR0	Propionyl-CoA carboxylase beta chain; mitochondrial OS = *B. taurus* GN = PCCB PE = 2 SV = 1
RG_G_Contig63	Metabolic	P21670	Proteasome subunit alpha type-4 OS = *Rattus norvegicus* GN = Psma4 PE = 1 SV = 1
RG_G_Contig12	Metabolic	Q9Z2I9	Succinyl-CoA ligase [ADP-forming] subunit beta; mitochondrial OS = *Mus musculus* GN = Sucla2 PE = 1 SV = 2
RG_C_Contig3	Metabolic	Q63569	26S protease regulatory subunit 6A OS = *R. norvegicus* GN = Psmc3 PE = 2 SV = 1
RG_C_Contig1	Metabolic	P08428	ATP synthase subunit alpha; mitochondrial OS = *Xenopus laevis* GN = atp5a PE = 2 SV = 1
RG_C_Contig2	Metabolic	P13184	Cytochrome c oxidase polypeptide 7A2; mitochondrial OS = *B. taurus* GN = COX7A2 PE = 1 SV = 3
RG_C_Contig81	Metabolic	P00430	Cytochrome c oxidase subunit 7C; mitochondrial OS = *B. taurus* GN = COX7C PE = 1 SV = 3
RG_C_Contig20	Metabolic	Q58DM8	Enoyl-CoA hydratase; mitochondrial OS = *B. taurus* GN = ECHS1 PE = 2 SV = 1
RG_C_Contig84	Metabolic	Q5XJ10	Glyceraldehyde 3-phosphate dehydrogenase; testis-specific OS = *Danio rerio* GN = gapdhs PE = 2 SV = 1
RG_C_Contig8	Metabolic	Q5NVR2	Malate dehydrogenase; mitochondrial OS = *Pongo abelii* GN = MDH2 PE = 2 SV = 1
RG_C_Contig48	Metabolic	Q4R4E0	NADH dehydrogenase [ubiquinone] 1 beta subcomplex subunit 5; mitochondrial OS = *M. fascicularis* GN = NDUFB5 PE = 2 SV = 1
RG_C_Contig28	Metabolic	P00480	Ornithine carbamoyltransferase; mitochondrial OS = *H. sapiens* GN = OTC PE = 1 SV = 3
RG_C_Contig26	Metabolic	Q5PQ01	Phosphatidylinositol-5-phosphate 4-kinase type-2 gamma OS = *X. laevis* GN = pip4k2c PE = 2 SV = 1
RG_C_Contig5	Metabolic	Q96IV6	Uncharacterized protein C5orf4 OS = *H. sapiens* GN = C5orf4 PE = 1 SV = 1
RG_K_Contig59	Metabolic	Q03248	Beta-ureidopropionase OS = *R. norvegicus* GN = Upb1 PE = 1 SV = 1
RG_K_Contig55	Metabolic	Q9N1E2	Glucose-6-phosphate isomerase OS = *Oryctolagus cuniculus* GN = GPI PE = 1 SV = 3
RG_K_Contig77	Metabolic	Q9UKU7	Isobutyryl-CoA dehydrogenase; mitochondrial OS = *H. sapiens* GN = ACAD8 PE = 1 SV = 1
RG_I_Contig19	Metabolic	Q9ER34	Aconitate hydratase; mitochondrial OS = *R. norvegicus* GN = Aco2 PE = 1 SV = 2
RG_I_Contig6	Metabolic	P06576	ATP synthase subunit beta; mitochondrial OS = *H. sapiens* GN = ATP5B PE = 1 SV = 3
RG_G_Contig5	Transport	Q9CZ13	Cytochrome b-c1 complex subunit 1; mitochondrial OS = *M. musculus* GN = Uqcrc1 PE = 1 SV = 1
RG_G_Contig20	Transport	Q9ZZ54	NADH-ubiquinone oxidoreductase chain 1 OS = *S. acanthias* GN = MT-ND1 PE = 3 SV = 1
RG_G_Contig70	Transport	Q6NRB0	Protein Hook homolog 2 OS = *X. laevis* GN = hook2 PE = 2 SV = 1
RG_C_Contig6	Transport	Q5E9B7	Chloride intracellular channel protein 1 OS = *B. taurus* GN = CLIC1 PE = 2 SV = 3
RG_C_Contig35	Transport	P00027	Cytochrome c OS = *Squalus suckleyi* GN = cyc PE = 1 SV = 2
RG_C_Contig45	Transport	Q62760	Mitochondrial import receptor subunit TOM20 homolog OS = *R. norvegicus* GN = Tomm20 PE = 1 SV = 2
RG_K_Contig15	Transport	P11442	Clathrin heavy chain 1 OS = *R. norvegicus* GN = Cltc PE = 1 SV = 3
RG_K_Contig2	Transport	Q8TAG9	Exocyst complex component 6 OS = *H. sapiens* GN = EXOC6 PE = 1 SV = 3
RG_G_Contig58	Process Regulation	P07737	Profilin-1 OS = *H. sapiens* GN = PFN1 PE = 1 SV = 2
RG_G_Contig29	Process Regulation	P35467	Protein S100-A1 OS = *R. norvegicus* GN = S100a1 PE = 1 SV = 3
RG_G_Contig39	Process Regulation	P46939	Utrophin OS = *H. sapiens* GN = UTRN PE = 1 SV = 2
RG_C_Contig25	Process Regulation	P63245	Guanine nucleotide-binding protein subunit beta-2-like 1 OS = *R. norvegicus* GN = Gnb2l1 PE = 1 SV = 3
RG_C_Contig14	Process Regulation	O42148	Ornithine decarboxylase antizyme OS = *Gallus gallus* GN = OAZ PE = 2 SV = 3
RG_C_Contig67	Process Regulation	P37805	Transgelin-3 OS = *R. norvegicus* GN = Tagln3 PE = 1 SV = 2
RG_K_Contig33	Process Regulation	Q9NPA3	Mid1-interacting protein 1 OS = *H. sapiens* GN = MID1IP1 PE = 1 SV = 1
RG_C_Contig4	Cell Death	P30405	Peptidyl-prolyl cis-trans isomerase; mitochondrial OS = *H. sapiens* GN = PPIF PE = 1 SV = 1
RG_K_Contig24	Cell Death	Q6DF07	Programmed cell death protein 10 OS = *Xenopus tropicalis* GN = pdcd10 PE = 2 SV = 1
RG_K_Contig52	Cell Death	Q9TT15	Voltage-dependent anion-selective channel protein 1 OS = *O. cuniculus* GN = VDAC1 PE = 2 SV = 3
RG_G_Contig35	Translation	Q6P8D1	40S ribosomal protein SA OS = *X. tropicalis* GN = rpsa PE = 2 SV = 1
RG_G_Contig22	Translation	P50878	60S ribosomal protein L4 OS = *R. norvegicus* GN = Rpl4 PE = 2 SV = 3
RG_C_Contig77	Translation	Q9BYC8	39S ribosomal protein L32; mitochondrial OS = *H. sapiens* GN = MRPL32 PE = 1 SV = 1
RG_C_Contig61	Translation	P41105	60S ribosomal protein L28 OS = *M. musculus* GN = Rpl28 PE = 1 SV = 2
RG_C_Contig69	Translation	P04646	60S ribosomal protein L35a OS = *R. norvegicus* GN = Rpl35a PE = 3 SV = 1
RG_C_Contig29	Translation	A5A6I3	Eukaryotic translation initiation factor 3 subunit F OS = Pan troglodytes GN = EIF3F PE = 2 SV = 1
RG_I_Contig15	Metabolic	Q90705	Elongation factor 2 OS = *G. gallus* GN = EEF2 PE = 1 SV = 3
RG_G_Contig25	RNA Processing	Q9ESX5	H/ACA ribonucleoprotein complex subunit 4 OS = *M. musculus* GN = Dkc1 PE = 1 SV = 3
RG_G_Contig54	RNA Processing	Q5XH16	NHP2-like protein 1 OS = *X. laevis* GN = nhp2l1 PE = 2 SV = 1
RG_C_Contig10	RNA Processing	P51991	Heterogeneous nuclear ribonucleoprotein A3 OS = *H. sapiens* GN = HNRNPA3 PE = 1 SV = 2
RG_C_Contig75	RNA Processing	Q06066	Nuclease-sensitive element-binding protein 1 OS = *G. gallus* GN = YBX1 PE = 2 SV = 1
RG_C_Contig36	RNA Processing	Q09167	Splicing factor; arginine/serine-rich 5 OS = *R. norvegicus* GN = Sfrs5 PE = 2 SV = 1
RG_G_Contig3	DNA Replication	Q4QQE9	Endonuclease-reverse transcriptase OS = *Schistosoma mansoni* PE = 2 SV = 1
RG_K_Contig40	DNA Replication	Q95SX7	Probable RNA-directed DNA polymerase from transposon BS OS = *Drosophila melanogaster* GN = RTase PE = 2 SV = 1
RG_K_Contig8	DNA Replication	P04323	Retrovirus-related Pol polyprotein from transposon 17.6 OS = *D. melanogaster* GN = pol PE = 4 SV = 1
RG_K_Contig75	Stress Response	Q58DR2	DnaJ homolog subfamily B member 12 OS = *B. taurus* GN = DNAJB12 PE = 2 SV = 1
RG_K_Contig5	Stress Response	P19120	Heat shock cognate 71 kDa protein OS = *B. taurus* GN = HSPA8 PE = 1 SV = 2
RG_C_Contig16	Calcium Binding	Q8VC88	Grancalcin OS = *M. musculus* GN = Gca PE = 2 SV = 1
RG_C_Contig78	Calcium Binding	Q5E984	Translationally-controlled tumor protein OS = *B. taurus* GN = TPT1 PE = 2 SV = 1
RG_G_Contig30	Structural	Q6P378	Actin; cytoplasmic 2 OS = *X. tropicalis* GN = actg1 PE = 2 SV = 1
RG_G_Contig27	Structural	O88342	WD repeat-containing protein 1 OS = *M. musculus* GN = Wdr1 PE = 1 SV = 3
RG_C_Contig43	Structural	P48649	Gamma-crystallin M2 OS = *Chiloscyllium colax* GN = GM2 PE = 2 SV = 2
RG_K_Contig47	Structural	Q90617	Lysosome-associated membrane glycoprotein 2 OS = *G. gallus* GN = LAMP2 PE = 2 SV = 1
RG_K_Contig22	Structural	Q64119	Myosin light polypeptide 6 OS = *R. norvegicus* GN = Myl6 PE = 1 SV = 3

Table 3 (*continued*)

Contig	Gene Ontology	Accession number	Description
a			
RG_K_Contig39	Structural	Q9QXS1	Plectin-1 OS = *M. musculus* GN = Plec1 PE = 1 SV = 2
RG_G_Contig68	Extracellular	Q8R3W7	Anterior gradient protein 3 homolog OS = *M. musculus* GN = Agr3 PE = 2 SV = 1
RG_G_Contig67	Cell Differentiation	Q6DEL2	Cleft lip and palate transmembrane protein 1 homolog OS = *D. rerio* GN = clptm1 PE = 2 SV = 1
RG_K_Contig41	Mitochondrial	A8KB87	Coiled-coil domain-containing protein 56 OS = *D. rerio* GN = ccdc56 PE = 3 SV = 1
RG_K_Contig1	Membrane	Q5R3Z8	F-box/LRR-repeat protein 2 OS = *P. abelii* GN = FBXL2 PE = 2 SV = 1
b			
RG_A_Contig24	Metabolic	P52209	6-Phosphogluconate dehydrogenase; decarboxylating OS = *H. sapiens* GN = PGD PE = 1 SV = 3
RG_A_Contig58	Metabolic	Q8QGP3	Carboxypeptidase Z OS = *G. gallus* GN = CPZ PE = 1 SV = 1
RG_A_Contig104	Metabolic	Q5RDE7	Cysteine desulfurase; mitochondrial OS = *P. abelii* GN = NFS1 PE = 2 SV = 1
RG_A_Contig115	Metabolic	P41320	Glutamine synthetase; mitochondrial OS = *S. acanthias* PE = 2 SV = 1
RG_A_Contig31	Metabolic	Q9ZZ53	NADH-ubiquinone oxidoreductase chain 2 OS = *S. acanthias* GN = MT-ND2 PE = 3 SV = 1
RG_A_Contig6	Metabolic	Q9ZZ54	NADH-ubiquinone oxidoreductase chain 3 OS = *S. acanthias* GN = MT-ND3 PE = 3 SV = 1
RG_A_Contig66	Metabolic	Q6AZB8	Putative nuclease HARBI1 OS = *D. rerio* GN = harbi1 PE = 2 SV = 1
RG_A_Contig8	Metabolic	Q92122	Pyruvate kinase muscle isozyme OS = *X. laevis* GN = pkm PE = 2 SV = 1
RG_A_Contig47	Metabolic	Q9YHT1	Succinate dehydrogenase [ubiquinone] flavoprotein subunit; mitochondrial OS = *G. gallus* GN = SDHA PE = 1 SV = 2
RG_E_Contig11	Metabolic	Q6PAB3	Malate dehydrogenase; cytoplasmic OS = *X. laevis* GN = mdh1 PE = 2 SV = 1
RG_E_Contig14	Metabolic	Q0MQ87	NADH dehydrogenase [ubiquinone] 1 alpha subcomplex subunit 12 OS = Pan troglodytes GN = NDUFA12 PE = 2 SV = 1
RG_E_Contig7	Metabolic	Q9HAB8	Phosphopantothenate-cysteine ligase OS = *H. sapiens* GN = PPCS PE = 1 SV = 2
RG_A_Contig62	Transport	Q5TZ80	Protein Hook homolog 1 OS = *D. rerio* GN = hook1 PE = 2 SV = 1
RG_A_Contig22	Transport	P05025	Sodium/potassium-transporting ATPase subunit alpha OS = Torpedo californica PE = 1 SV = 1
RG_A_Contig46	Transport	Q92030	Sodium/potassium-transporting ATPase subunit alpha-1 OS = *A. anguilla* GN = atp1a1 PE = 2 SV = 1
RG_A_Contig11	Transport	B5DEN9	Vacuolar protein sorting-associated protein 28 homolog OS = *R. norvegicus* GN = Vps28 PE = 2 SV = 1
RG_E_Contig4	Transport	Q9D0F3	Protein ERGIC-53 OS = *M. musculus* GN = Lman1 PE = 2 SV = 1
RG_E_Contig13	Transport	Q4QQS3	Protein OSCP1 OS = *R. norvegicus* GN = Oscp1 PE = 2 SV = 1
RG_A_Contig35	Process Regulation	A6QNS3	Active breakpoint cluster region-related protein OS = *B. taurus* GN = ABR PE = 2 SV = 1
RG_A_Contig40	Process Regulation	P20111	Alpha-actinin-2 OS = *G. gallus* GN = ACTN2 PE = 2 SV = 1
RG_A_Contig2	Process Regulation	Q9QXT1	Dual adapter for phosphotyrosine and 3-phosphotyrosine and 3-phosphoinositide OS = *M. musculus* GN = Dapp1 PE = 1 SV = 1
RG_A_Contig36	Process Regulation	Q5RB37	Inter-alpha-trypsin inhibitor heavy chain H3 OS = *P. abelii* GN = ITIH3 PE = 2 SV = 1
RG_A_Contig102	Process Regulation	Q13526	Peptidyl-prolyl cis-trans isomerase NIMA-interacting 1 OS = *H. sapiens* GN = PIN1 PE = 1 SV = 1
RG_A_Contig26	Process Regulation	P69735	Rab3 GTPase-activating protein catalytic subunit (Fragments) OS = *R. norvegicus* GN = Rab3gap1 PE = 1 SV = 2
RG_A_Contig12	Process Regulation	O00560	Syntenin-1 OS = *H. sapiens* GN = SDCBP PE = 1 SV = 1
RG_E_Contig6	Process Regulation	P06238	Alpha-2-macroglobulin OS = *R. norvegicus* GN = A2m PE = 2 SV = 2
RG_A_Contig94	Cell Death	Q95M17	Acidic mammalian chitinase OS = *B. taurus* GN = CHIA PE = 1 SV = 1
RG_A_Contig59	Cell Death	B2GV05	RNA-binding protein 5 OS = *R. norvegicus* GN = Rbm5 PE = 2 SV = 1
RG_A_Contig97	Translation	P12749	60S ribosomal protein L26 OS = *R. norvegicus* GN = Rpl26 PE = 1 SV = 1
RG_A_Contig57	Translation	P81795	Eukaryotic translation initiation factor 2 subunit 3 OS = *R. norvegicus* GN = Eif2s3 PE = 1 SV = 2
RG_A_Contig7	Translation	Q641X8	Eukaryotic translation initiation factor 3 subunit E OS = *R. norvegicus* GN = Eif3e PE = 2 SV = 1
RG_A_Contig54	RNA Processing	Q9CWY4	Gem-associated protein 7 OS = *M. musculus* GN = Gemin7 PE = 2 SV = 1
RG_A_Contig92	DNA Replication	Q4QQE9	Endonuclease-reverse transcriptase OS = *S. mansoni* PE = 2 SV = 1
RG_A_Contig98	DNA Replication	P21328	RNA-directed DNA polymerase from mobile element jockey OS = *D. melanogaster* GN = pol PE = 1 SV = 1
RG_A_Contig69	Transcription	A0JN61	DNA-directed RNA polymerase III subunit RPC9 OS = *B. taurus* GN = CRCP PE = 2 SV = 1
RG_A_Contig48	Transcription	Q2T9L9	General transcription factor IIF subunit 2 OS = *B. taurus* GN = GTF2F2 PE = 2 SV = 1
RG_A_Contig89	Transcription	Q1KKY3	Homeobox protein Hox-B13a OS = *T. rubripes* GN = hoxb13a PE = 3 SV = 1
RG_A_Contig109	Transcription	Q28C74	Leucine-rich PPR motif-containing protein; mitochondrial OS = *X. tropicalis* GN = lrpprc PE = 2 SV = 1
RG_A_Contig28	Transcription	Q64152	Transcription factor BTF3 OS = *M. musculus* GN = Btf3 PE = 2 SV = 3
RG_A_Contig85	Structural	Q5ZJ81	Endophilin-B2 OS = *G. gallus* GN = SH3GLB2 PE = 2 SV = 1
RG_A_Contig110	Structural	Q5ZLA6	Myosin-Ic OS = *G. gallus* GN = MYO1C PE = 2 SV = 1
RG_A_Contig78	Structural	Q28IX8	Tubulin alpha chain OS = *X. tropicalis* GN = tuba PE = 2 SV = 1
RG_E_Contig2	Structural	P02460	Collagen alpha-1(II) chain (Fragment) OS = *G. gallus* GN = COL2A1 PE = 2 SV = 1
RG_A_Contig1	Iron Storage	Q95MP7	Ferritin heavy chain OS = *Canis familiaris* GN = FTH1 PE = 2 SV = 3
RG_A_Contig14	Calcium Binding	Q641Z8	Peflin OS = *R. norvegicus* GN = Pef1 PE = 2 SV = 1
RG_A_Contig9	Ubiquitination	Q8R3P2	Protein deltex-2 OS = *M. musculus* GN = Dtx2 PE = 1 SV = 2
RG_A_Contig15	Cell Communication	A8WCF8	Tumor protein p63-regulated gene 1-like protein OS = *R. norvegicus* GN = Tprg1l PE = 1 SV = 1
RG_A_Contig82	Platelet Adhesion	Q28833	von Willebrand factor (Fragment) OS = *Sus scrofa* GN = VWF PE = 2 SV = 2
RG_E_Contig16	Cell Proliferation	P47974	Butyrate response factor 2 OS = *H. sapiens* GN = ZFP36L2 PE = 1 SV = 3
RG_E_Contig15	DNA Ligation	P12682	High mobility group protein B1 OS = *S. scrofa* GN = HMGB1 PE = 2 SV = 3
RG_A_Contig61	Nucleus	Q96A49	Synapse-associated protein 1 OS = *H. sapiens* GN = SYAP1 PE = 1 SV = 1
RG_A_Contig18	Membrane	O95857	Tetraspanin-13 OS = *H. sapiens* GN = TSPAN13 PE = 2 SV = 1
RG_A_Contig5	Membrane	Q9NRQ5	UPF0443 protein C11orf75 OS = *H. sapiens* GN = C11orf75 PE = 2 SV = 1

4. Final perspectives

Many of the categories of genes (e.g., metabolism, transport, morphological/structural), and many genes in particular, whose transcripts were up regulated by feeding and activation of the rectal gland were in fact expected. Strikingly though, transcripts for many genes in these same categories were up regulated during fasting, and in several cases appear to be out of phase with previously reported increases in enzyme activities and protein contents during activation of the gland during feeding. A reasonable explanation for this phase variance is that the gland stores mRNA during fasting for selected genes in 'anticipation' of the need for rapid synthesis of selected proteins immediately upon feeding. Given the growing body of evidence for the role of microRNA regulation of mRNA availability for translation (Cai et al., 2009), it would be of interest to examine their role in the regulation of rectal gland function in elasmobranchs.

Supplementary data to this article can be found online at http://dx.doi.org/10.1016/j.cbd.2013.09.003.

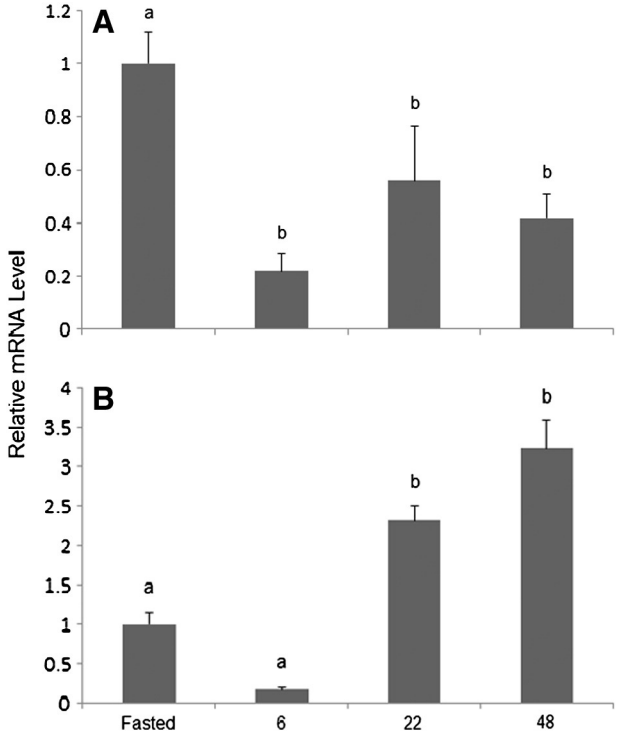

Fig. 2. Real time quantitative PCR analysis of relative transcript abundance in rectal glands of fed (6, 22 and 48 h) relative to 7 day fasted (ratio set at 1.0) spiny dogfish (*Squalus acanthias*) for (A) glutamine synthetase and (B) cytochrome c oxidase compared to expression of elongation factor 1 alpha as the reference gene. Values are means ± 1 S.E.M., and those with different letters are statistically different ($p < 0.05$ by ANOVA).

Acknowledgments

We wish to thank the members of the Bamfield Marine Sciences Centre support staff for their logistic support. We thank Dr. Andy Gracey for advice on Normalized cDNA library construction, and Drs. Diego Fiol, Dietmar Kultz and Frank Melzner for advice on SSH. This research was supported by Discovery Grants from the Natural Sciences and Engineering Council of Canada to CMW and PJW, both of whom are also supported by the Canada Research Chair Program.

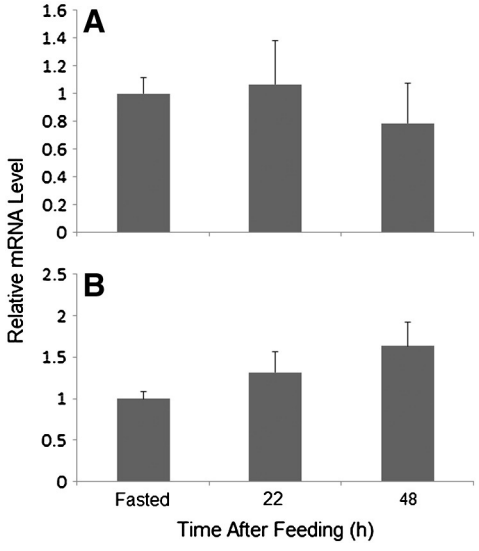

Fig. 3. Real time quantitative PCR analysis of relative transcript abundance in rectal glands of fed (22 and 48 h) relative to fasted (ratio set at 1.0) spiny dogfish (*Squalus acanthias*) for (A) Na^+/K^+-ATPase and (B) lactate dehydrogenase compared to expression of elongation factor 1 alpha as the reference gene. Values are means ± 1 S.E.M., and there were no significant differences among treatments.

References

Altschul, S.F., Madden, T.L., Schaffer, A.A., Zhang, J., Zhang, Z., Miller, W., Lipman, D.J., 1997. Gapped BLAST and PSI-BLAST: a new generation of protein database search programs. Nucleic Acids Res. 25, 3389–3402.

Anderson, W.G., Taylor, J.R., Good, J.P., Hazon, N., Grosell, M., 2007. Body fluid volume regulation in elasmobranch fish. Comp. Biochem. Physiol. A 148, 3–13.

Armour, K.J., O'Toole, L.B., Hazon, N., 1993. The effect of dietary protein restriction on the secretory dynamics of 1α-hydroxycorticosterone and urea in the dogfish, *Scyliorhinus canicula*: a possible role for 1α-hydroxycorticosterone in sodium retention. J. Endocrinol. 138, 275–282.

Boguski, M.S., Lowe, T.M., Tolstoshev, C.M., 1993. dbEST—database for "expressed sequence tags". Nat. Genet. 4, 332–333.

Bystriansky, J.S., Richards, J.G., Schulte, P.M., Ballantyne, J.S., 2006. Reciprocal expression of gill Na^+/K^+-ATPase a-subunit isoforms a1a and a1b during seawater acclimation of three salmonid fishes that vary in their salinity tolerance. J. Exp. Biol. 209, 1848–1858.

Cai, Y., Xiaomin, Y., Yu, J., 2009. A brief review on the mechanisms of miRNA regulation. Genomics Proteomics Bioinformatics 7, 147–154.

Diatchenko, L., Lau, Y.F.C., Campbell, A.P., Chenchik, A., Moqadam, F., et al., 1996. Suppression subtractive hybridization: a method for generating differentially regulated or tissue-specific cDNA probes and libraries. Proc. Natl. Acad. Sci. U. S. A. 93, 6025–6030.

Dowd, W.W., Wood, C.M., Kajimura, M., Walsh, P.J., Kültz, D., 2008. Natural feeding influences protein expression in the dogfish shark rectal gland: a proteomic analysis. Comp. Biochem. Physiol. D 3, 118–127.

Ebert, D.A., White, W.T., Goldman, K.J., Compagno, L.J.V., Daly-Engel, T.S., Ward, R.D., 2010. Resurrection and redescription of *Squalus suckleyi* Girard from the North Pacific, with comments on the *Squalus acanthias* subgroup (Squaliformes: Squalidae). Zootaxa 2612, 22–40.

Epstein, F.H., Stoff, J.S., Silva, P., 1983. Mechanism and control of hyperosmotic NaCl-rich secretion by the rectal gland of *Squalus acanthias*. J. Exp. Biol. 106, 25–41.

Ewing, B., Green, P., 1998. Base-calling of automated sequencer traces using phred. II. Error probabilities. Genome Res. 8, 186–194.

Ewing, B., Hillier, L., Wendl, M.C., Green, P., 1998. Base-calling of automated sequencer traces using Phred. I. Accuracy assessment. Genome Res. 8, 175–185.

Fiedler, T.J., Hudder, A., McKay, S.J., Shivkumar, S., Capo, T.R., Schmale, M.C., Walsh, P.J., 2010. The transcriptome of early life history stages of the California sea hare, *Aplysia californica*. Comp. Biochem. Physiol. D 5, 165–170.

Fiol, D.F., Chan, S.Y., Kültz, D., 2006. Identification and pathway analysis of immediate hyperosmotic stress responsive molecular mechanisms in tilapia (*Oreochromis mossambicus*) gill. Comp. Biochem. Physiol. D 1, 344–356.

Gracey, A.Y., Troll, J.V., Somero, G.N., 2001. Hypoxia-induced gene expression profiling in the euryoxic fish *Gillichthys mirabilis*. Proc. Natl. Acad. Sci. U. S. A. 98, 1993–1998.

Haywood, G.P., 1973. Hypo-osmotic regulation coupled with reduced metabolic urea in dogfish *Poroderma africanum*: an analysis of serum osmolarity, chloride, and urea. Mar. Biol. 23, 121–127.

Helmstetter, C., Pope, R.K., T'Flachebba, M., Secor, S.M., Lignot, J.-H., 2009. The effects of feeding on cell morphology and proliferation of the gastrointestinal tract of juvenile Burmese pythons (*Python molurus*). Can. J. Zool. 87, 1255–1267.

Huang, X., Madan, A., 1999. CAP3: a DNA sequence assembly program. Genome Res. 9, 868–877.

Kajimura, M., Walsh, P.J., Wood, C.M., 2008. The dogfish shark (*Squalus acanthias*) maintains osmolyte balance during long-term starvation. J. Fish Biol. 72, 656–670.

Kanehisa, M., Araki, M., Goto, S., Hattori, M., Hirakawa, M., Itoh, M., Katayama, T., Kawashima, S., Okuda, S., Tokimatsu, T., Yamanishi, Y., 2008. KEGG for linking genomes to life and the environment. Nucleic Acids Res. 36, D480–D484.

Lignot, J.-H., Helmstetter, C., Secor, S.M., 2005. Postprandial morphological response of the intestinal epithelium of the Burmese python (*Python molurus*). Comp. Biochem. Physiol. A 141, 280–291.

MacKenzie, S., Cutler, C.P., Hazon, N., Cramb, G., 2002. The effects of dietary sodium loading on the activity and expression of Na, K-ATPase in the rectal gland of the European dogfish (*Scyliorhinus canicula*). Comp. Biochem. Physiol. B 131, 185–200.

Mahmmoud, Y.A., Vorum, H., Cornelius, F., 2000. Identification of a Phospholemman-like protein from shark rectal glands: evidence for indirect regulation of Na-K-ATPase by protein kinase C via a novel member of the FXYD family. J. Biol. Chem. 275, 35969–35977.

Matey, V., Wood, C.M., Dowd, W., Kültz, D., Walsh, P.J., 2009. Morphology of the rectal gland of the spiny dogfish (*Squalus acanthias*) shark in response to feeding. Can. J. Zool. 87, 440–452.

Oleksiak, M.F., Kotell, K.J., Crawford, D.L., 2001. Utility of natural populations for microarray analyses: isolation of genes necessary for functional genomic studies. Mar. Biotechnol. 3, S203–S211.

Olson, K.R., 1999. Rectal gland and volume homeostasis. In: Hamlett, W.C. (Ed.), Sharks, Skates, and Rays. Johns Hopkins University Press, Baltimore. MD, pp. 329–352.

Richards, J.G., Semple, J.W., Bystriansky, J.S., Schulte, P.M., 2003. Na^+/K^+-ATPase a-isoform switching in gills of rainbow trout (*Oncorhynchus mykiss*) during salinity transfer. J. Exp. Biol. 206, 4475–4486.

Schmid, R., Blaxter, M.L., 2008. annot8r: rapid assignment of GO, EC and KEGG annotations. BMC Bioinforma. 9, 180.

Schofield, J.P., Jones, D.S., Forrest, J.N., 1991. Identification of C-type natriuretic peptide in heart of spiny dogfish shark (*Squalus acathias*). Am. J. Physiol. 261, F734–F739.

Shuttleworth, T.J., Thompson, J., Munger, S.R., Wood, C.M., 2006. Respiratory gas exchange, carbonic anhydrase function and acid–base control of secretion in the isolated-perfused rectal gland of *Squalus acanthias*. J. Exp. Biol. 209, 4701–4706.

Silva, P., Solomon, R.J., Epstein, F.H., 1997. Transport mechanisms that mediate the secretion of chloride by the rectal gland of *Squalus acanthias*. J. Exp. Zool. 279, 504–508.

Solomon, R.J., Taylor, M., Rosa, R., Silva, P., Epstein, F.H., 1984. In vivo effect of volume expansion on rectal gland function. II. Hemodynamic changes. Am. J. Physiol. 246, R67–R71.

Staden, R., 1980. A new computer method for the storage and manipulation of DNA gel reading data. Nucleic Acids Res. 8, 3673–3694.

Stajich, J.E., Block, D., Boulez, K., Brenner, S.E., Chervitz, S.A., Dagdigian, C., Fuellen, G., Gilbert, J.G.R., Korf, Lapp, H., Lehvaslaiho, H., Matsalla, C., Mungall, C.J., Osborne, B., Pocock, M.R., Schattner, Senger, M., Stein, L.D., Stupka, E., Wilkinson, M.D., Birney, E., 2002. The Bioperl Toolkit: Perl modules for the life sciences. Genome Res. 12, 1611–1618.

The Gene Ontology Consortium, 2000. Gene Ontology: tool for the unification of biology. Nat. Genet. 25, 25–29.

The UniProt Consortium, 2008. The Universal Protein Resource (UniProt). Nucleic Acids Res. 36, D190–D195.

Walsh, P.J., Kajimura, M., Mommsen, T.P., Wood, C.M., 2006. Metabolic organization and effects of feeding on enzyme activities of the dogfish shark (*Squalus acanthias*) rectal gland. J. Exp. Biol. 209, 2929–2938.

Wheeler, D.L., Chappey, C., Lash, A.E., Leipe, D.D., Madden, T.L., Schuler, G.D., Tatusova, T.A., Rapp, B.A., 2000. Database resources of the National Center for Biotechnology Information. Nucleic Acids Res. 28, 10–14.

Wood, C.M., Kajimura, M., Mommsen, T.P., Walsh, P.J., 2005. Alkaline tide and nitrogen conservation after feeding in the elasmobranch *Squalus acanthias*. J. Exp. Biol. 208, 2693–2705.

Wood, C.M., Kajimura, M., Bucking, C.P., Walsh, P.J., 2007a. Osmoregulation, ionoregulation, and acid–base regulation by the gastrointestinal tract after feeding in the dogfish shark. J. Exp. Biol. 210, 1335–1349.

Wood, C.M., Munger, S.R., Thompson, J., Shuttleworth, T.J., 2007b. Control of rectal gland secretion by blood acid–base status in the intact dogfish shark (*Squalus acanthias*). Respir. Physiol. Neurobiol. 156, 220–228.

Wood, C.M., Walsh, P.J., Kajimura, M., McClelland, G.C., Chew, S.F., 2010. The influence of feeding and fasting on plasma metabolites in the dogfish shark (*Squalus acanthias*). Comp. Biochem. Physiol. A 155, 435–444.